RSC Advances

This is an *Accepted Manuscript*, which has been through the Royal Society of Chemistry peer review process and has been accepted for publication.

Accepted Manuscripts are published online shortly after acceptance, before technical editing, formatting and proof reading. Using this free service, authors can make their results available to the community, in citable form, before we publish the edited article. This *Accepted Manuscript* will be replaced by the edited, formatted and paginated article as soon as this is available.

You can find more information about *Accepted Manuscripts* in the **Information for Authors**.

ROYAL SOCIETY OF CHEMISTRY

www.rsc.org/advances

Graphical abstract

Three complexes were synthesized and characterized. The cytotoxicity, apoptosis, cellular uptake, reactive oxygen species, mitochondrial membrane potential, cell cycle arrest and western blot analysis were investigated.
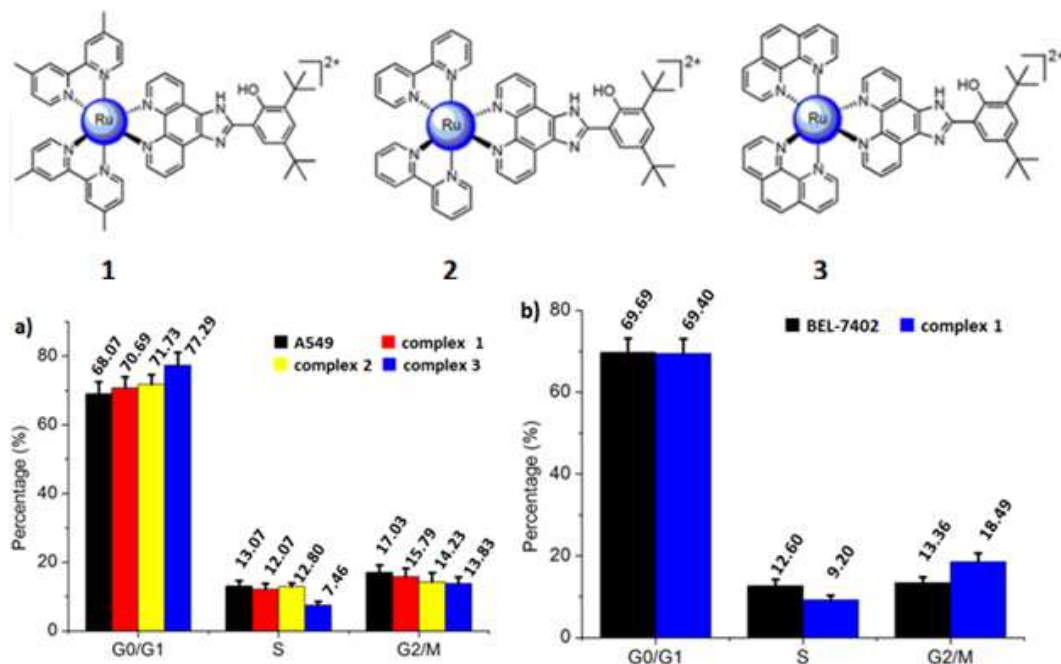
Submitted to RSC Advances

The Studies on Bioactivity in Vitro of Ruthenium(II) Polypyridyl Complexes Towards Human Lung Carcinoma A549 cells

Bing-Jie Han[a], Guang-Bin Jiang[a], Ji Wang[a], Wei Li[a], Hong-Liang Huang[b],*,

Yun-Jun Liu[a],*

[a]*School of Pharmacy, Guangdong Pharmaceutical University, Guangzhou, 510006, P.R. China*

[b]*School of Life Science and Biopharmaceutical, Guangdong Pharmaceutical University, Guangzhou, 510006, P.R. China*

* Corresponding author. Tel: +86 20 39352122; fax: +86 20 39352128

E-mail address: hhongliang@163.com (H.L. Huang), lyjche@163.com(Y.J. Liu)

Abstract: Three Ru(II) polypyridyl complexes [Ru(dmb)$_2$(HDPIP)](ClO$_4$)$_2$ (**1**), [Ru(bpy)$_2$(HDPIP)](ClO$_4$)$_2$ (**2**) and [Ru(phen)$_2$(HDPIP)](ClO$_4$)$_2$ (**3**) were synthesized and characterized. The IC$_{50}$ values of the complexes against BEL-7402, A549, MG-63 and SK-BR-3 cells range from 20.8 ± 1.6 to 7.3 ± 1.0 µM. Complexes **1**, **2** and **3** can enhance the ROS levels and enter into the cytoplasm and accumulate in the cell nuclei. All the complexes can induce the decrease of the mitochondrial membrane potential and inhibit the cell growth in A549 cells at G0/G1 phase. Complex **3** has no obvious impact on the expression of the anti-apoptotic protein Bcl-2, and increases the levels of the pro-apoptotic proteins Bax and Bid. Complex **3** induces apoptosis of A549 cells through ROS-mediated mitochondrial dysfunction pathway.

1. Introduction

The serious side effects such as neurotoxicity and nephrotoxicity of cisplatin have limited its clinical application [1,2]. Thus the search for new metal complexes with high cytotoxic activity against cancer cells is an important field of research. Previously, a number of ruthenium compounds have been shown to display promising anticancer activity [3-10]. Two Ru(II) complexes have successfully entered clinical trials, namely, NAMI-A ([ImH][*trans*-RuCl$_4$ (DMSO)(Im)], where Im = imidazole and DMSO = dimethylsulfoxide) [11] and KP1019 ([IndH][*trans*-RuCl$_4$(Ind)$_2$], where

Ind = indazole [12]. In recent years, ruthenium complexes have received considerable interest in bioactivity [13-20]. Complex $[Ru(phen)_2(mdpz)]^{2+}$ is able to enhance the stability of the RNA triplex Poly(U)·Poly(A)·Poly(U) and serve as a prominent molecular ″light switch″ for the RNA triplex [21]. $[Ru(phen)_2(P\text{-}MOPIP)]^{2+}$ shows high cytotoxic activity against A549 cells with a low IC_{50} value of 5.9 ± 1.1 μM, and can induce mitochondria-mediated and caspase-dependent apoptosis in human cancer cells [22]. H_2-β-ethynyltetraphenylporphyrin-Ru(phen)-(bpy)$_2$Cl$_2$ exhibits rapid cellular uptake, low dark-cytotoxicity, and high photo-cytotoxicity toward HK-1 (human nasopharyngeal carcinoma) and HeLa (cervical carcinoma) cells [23]. Complex $[Ru(dip)_2(PAIDH)]^{2+}$ (dip = 4,7-dimethyl-1,10-phenanthroline, PAIDH = 2-pyridyl-1H-anthra[1,2-d]imidazole-6,11-dione) was shown to accumulate preferentially in the mitochondria of HeLa cells and induced apoptosis via the mitochondrial pathway, which involved ROS generation, mitochondrial membrane potential depolarization [24], complex $[Ru(phen)_2(addppn)]^{2+}$ shows very high inhibitory effect against BEL-7402 cells ($IC_{50} = 3.9 \pm 0.4$ μM) [25]. In our previous work [26,27], we found that ruthenium(II) complexes with polypyridyl ligand containing hydroxyl group have high cytotoxic activity against tumor cell lines. In order to obtain more insight into the bioactivity of this kind ruthenium complexes, in this report, we synthesized and characterized three ruthenium(II) complexes with hydroxyl group as substituent group, $[Ru(dmb)_2(HDPIP)](ClO_4)_2$ (**1**) (HDPIP = 2-(2-hydroxyl-3,5-ditert-butylphenyl)imidazo[4,5-f][1,10]phenanthroline, dmb = 4,4'-dimethyl-2,2'-bipyridine), $[Ru(bpy)_2(HDPIP)](ClO_4)_2$ (**2**) (bpy = 2,2'-bipyridine)

3

and [Ru(phen)$_2$(HDPIP)](ClO$_4$)$_2$ (**3**) (phen = 1,10-phenanthroline, Scheme 1). Their

cytotoxicity in vitro against BEL-7402, A549, MG-63 and SK-BR-3 cells was

evaluated by 3-(4,5-dimethylthiazol-2-yl)-2,5-diphenyltetrazolium (MTT) assay. The

morphological apoptosis of A549 cells induced by these complexes was investigated

with fluorescent microscope. The reactive oxygen species (ROS) and mitochondrial

membrane potential were assayed by fluorescence microscopy and microplate

analyzer. The cell cycle distribution of A549 and BEL-7402 cells was investigated by

flow cytometry. The apoptotic mechanism was also investigated in detail by western

blot analysis.

2. Results and discussion

2.1. Synthesis and characterization

The ligand HDPIP was easily synthesized following the method described in the

literature. The complexes **1**, **2** and **3** were obtained by refluxing relative precursor

with HDPIP in ethanol. The synthesized complexes were characterized by ^{1}H NMR,

ES-MS and elemental analysis. In the ES-MS spectra for the Ru(II) complexes, all of

the expected signals [M-2ClO$_4$-H]$^+$, and [M-2ClO$_4$]$^{2+}$ were observed. The measured

molecular weights were consistent with the expected values.

2.2. Cytotoxic Activity in Vitro Assay

The cell viability was determined by MTT method and the IC$_{50}$ values are listed in

Table 1. All the four tumor cell lines i.e. BEL-7402, A549, MG-63 and SK-BR-3,

4

showed differential effect on killing cells with increasing concentrations of complexes **1**, **2** and **3**. Among the four cell lines, A549 was found to be most sensitive, while MG-63 was relatively less sensitive to the complexes. Comparing the IC_{50} values, complex **3** shows the highest cytotoxic activity against A549 cells among the three complexes under the same conditions. Moreover, complex **3** exhibits comparable cytotoxic effect with ciaplatin on A549 cells. Complex **2** displays the same cytotoxic activity as complex **3** toward SK-BR-3 cells. Complex **1** shows relative higher inhibitory effect than **2** and **3** on BEL-7402 cells. The cytotoxic activity of these complexes is lower than those of the $[Ru(phen)_2(addppn)]^{2+}$ reported in our previous work [25] and $[Ru(Nap-etsc)(CO)(PPh_3)_2]\cdot Cl$ ($IC_{50} = 2.0 \pm 0.2$ μM) against A549 cells [28]. Obviously, different complexes exhibit different cytotoxic activity against the different tumor cell lines. Complexes **1**, **2** and **3** are sensitive to A549 cells, thus, this cell line was selected in the following experiments.

2.3. Apoptotic studies by AO/EB staining method

The apoptotic assay of A549 cells induced by complexes **1**, **2** and **3** was performed using acridine orange (AO) and ethidium bromide (EB) staining method. It is well known that AO is a vital dye and can stain both live and dead cells. EB stains only cells that have lost their membrane integrity. On the basis of overall cell morphology and cell membrane integrity, necrotic and apoptotic cells can be distinguished from one another using fluorescence microscope. In the control (Fig. 1a), the living cells are stained bright green in spots. However, A549 cells were exposed to 12.5 μM of

5

complexes **1**, **2** and **3** for 24 h (Fig. 1b-1d), apoptotic cells appear green and contain apoptotic characteristics such as cell blebbing, nuclear shrinkage and chromatin condensation, and necrotic cells show red. These characteristics indicate that these complexes can induce apoptosis of A549 cells.

2.4. Cellular Uptake and Co-location Studies

The cellular uptake is an important factor that usually contributes to transition metal-based drug cytotoxicity [29]. Many ruthenium complexes can be uptaken by various cancer cells [30-33]. Complexes **1**, **2** and **3** uptaken by A549 cells was investigated under fluorescence microscope. After A549 cells were exposed to 25 μM of complexes **1**, **2** and **3** for 24 h, the cellular uptake effect is shown in Fig. 2. The blue channel shows DAPI-stained nuclei with an excitation wavelength of 340 nm, the red channel indicates the luminescence of complexes **1**, **2** and **3** with an excitation wavelength of 458 nm, and the overlay displays cellular association of **1**, **2** and **3**. The results indicates that complexes **1**, **2** and **3** are successfully uptaken by A549 cells and these Ru(II) complexes can enter into the cytoplasm and accumulate in the nuclei.

2.5. Effects of the Complexes on Reactive Oxygen Species (ROS) levels

Reactive oxygen species (ROS) are known to affect mitochondrial membrane potential and trigger a series of mitochondria associated events including apoptosis [34]. Role of ROS as mediators of apoptosis is becoming increasingly recognized. Many potential anticancer and chemopreventive agents induce apoptosis through ROS

generation [35]. It is well known that $H_2DCF\text{-}DA$ (2',7'-dichlorodihydrofluorescein diacetate) is a cell-permeant dye and is cleaved by intracellular esterase into its non-fluorescent form (DCFH). DCFH is oxidized by intracellular free radicals to produce a fluorescent product DCF (dichlorofluorescein) [36,37]. The fluorescent intensity of DCF is shown in Fig. 3. The DCF fluorescence intensity increased significantly when the A549 cells were exposed to different concentrations of complexes **1**, **2** or **3**. The treatment with 6.25 μM of complexes **1**, **2** or **3** resulted in a 1.41, 1.49 and 1.27-fold increase in the fluorescent intensity compared with the control, respectively. These results show that these complexes can enhance the levels of ROS.

2.6. Detection of Mitochondrial Membrane Potential

After A549 cells were exposed to different concentrations of complexes **1**, **2** or **3** for 24 h, mitochondrial dysfunction was assayed with JC-1 (5,5',6,6'-tetrachloro-1,1',3,3'-tetrethylbenzimidalylcarbocyanine iodide) as fluorescent probe. JC-1 monomer emits green fluorescence signals corresponding to low membrane potential. At high membrane potential, JC-1 aggregate shows red fluorescence signals. As shown in Fig. 4, in the control (Fig. 4a), JC-1 emits red fluorescence (JC-aggregates). Treatment of A549 cells with 12.5 μM complexes **1** (b), **2** (c) and **3** (d) for 24 h, JC-1 displays a green with little red fluorescence (JC-1 monomers). The change from red to green fluorescence indicates the decrease of mitochondrial membrane potential. The change of mitochondrial membrane potential

7

was also detected by determining the ratio of the red and green fluorescent intensity with microplate analyzer. As shown in Fig. 5, in the control, the ratio of red/green is 29.41, A549 cells exposure to 12.5 or 25 μM of complexes **1**, **2** and **3** for 24 h, the ratios of red/green are 18.91 and 12.37 for **1**, 26.61 and 22.86 for **2**, 20.52 and 10.59 for **3**, respectively. Comparing the ratio values, at 25 μM, complex **3** induces much reduction in mitochondrial membrane potential than complexes **1** and **2** under identical conditions. The reduction of red/green values suggests that red fluorescent intensity decreases and green fluorescent intensity increases. These results also indicate that the complexes can induce the decrease of mitochondrial membrane potential and causes mitochondrial dysfunction. Furthermore, the reduction of mitochondrial membrane potential induced by the complexes is concentration-dependent.

2.7. Cell Cycle Arrest Studies

Inhibition of cancer cell proliferation by cytotoxic drugs could be the result of induction of apoptosis or cell cycle arrest or a combination of these. The effect of complexes **1**, **2** and **3** on the cell cycle in A549 and BEL-7402 cells was studied by flow cytometry in propidium iodide (PI)-stained cells after Ru(II) complex treatment for 24 h. As shown in Fig. 6, for A549 cells (Fig. 6a), in the control, the percentage of G0/G1 phase is 68.97%, A549 cells exposure to 12.5 μM of complexes **1**, **2** and **3**, the percentages of G0/G1 phase are 70.69%, 71.73% and 77.29%, respectively. The enhancement of 1.72%, 2.76% and 8.32% for **1**, **2** and **3** in the percentage at G0/G1

phase was observed, accompanied by corresponding reduction in the percentage at S and G2/M phases. Furthermore, complex **3** shows larger inhibitory effect than complexes **1** and **2** on A549 cell cycle under the same conditions. These results suggest that complexes **1**, **2** and **3** induce cell cycle arrest in A549 cells at G0/G1 phase. After the treatment of BEL-7402 cells with complex **1** (Fig. 6b), the large increase of 5.13% in the percentage of cells at S phase was observed. The increase in S phase indicates that the antiproliferative mechanism induced by complex **1** in BEL-7402 cells is S-phase arrest. These results also show that the identical complex displays different antiproliferative mechanism toward different tumor cells.

2.8. Western Blot Analysis

Complex **3** shows the highest cytotoxic activity against A549 cells among the three complexes, thus this complex was selected for western blot analysis. The effects of complex **3** on the protein expression of procaspase 3, procaspase 7, caspase 7 and caspase 9 in A549 cells are shown in Fig. 7A. Treatment of A549 cells with 6.25, 12.5 and 25 μM of complex **3** for 24 h resulted in an increases in the expression levels of paocaspase 3, caspase 7 and caspase 9. However, no obvious change in the level of procaspase 7 expression was observed. The Bcl-2 family of proteins has been determined to be involved in apoptosis, including the pro-apoptotic protein Bax and the anti-apoptotic protein Bcl-2. Moreover, the ratio of Bcl-2 to Bax is a decisive factor that plays an important role in determining whether cells will undergo apoptosis under experimental conditions that promote cell death [38]. The effects of complex **3**

9

on the protein expression of the Bcl-2 family are shown in Fig. 7B. Treatment with different concentrations of **3** caused no obvious change in the levels of expression of the anti-apoptosis protein Bcl-2, and the expression levels of the pro-apoptosis proteins Bax and Bid increased. The ratios of Bcl-2/Bax and Bcl-2/Bid decreased significantly, leading to a generation of ROS, a depletion of mitochondrial membrane potential.

3. Conclusion

In summary, we synthesized three ruthenium(II) polypyridyl complexes. These complexes can effectively induce A549 cells apoptosis, and they can enter into cytoplasm and accumulate in the nuclei. ROS and mitochondrial membrane potential show that complexes **1**, **2** and **3** can enhance the reactive oxygen species levels and decrease the mitochondrial membrane potential. Additionally, complex **3** can activate procaspase 3, caspase 7 and 9, upregulate the expression levels of proapoptotic proteins Bax and Bid. These studies suggest that complex **3** induces apoptosis in A549 cells through ROS-mediated mitochondrial dysfunction pathway.

4. Experimental Section

4.1. Materials and method

All reagents and solvents were of commercial origin and were used without further purification unless otherwise noted. Ultrapure MilliQ water was used in all experiments. DMSO and RPMI 1640 were purchased from Sigma. Cell lines of

BEL-7402 (Hepatocellular), A549 (Human lung carcinoma), MG-63 (Human osteosarcoma) and SK-BR-3 (Human breast cancer) were purchased from the American Type Culture Collection. $RuCl_3 \cdot 3H_2O$ was purchased from the Kunming Institution of Precious Metals. 1,10-phenanthroline was obtained from the Guangzhou Chemical Reagent Factory.

Microanalyses (C, H, and N) were obtained with a Perkin-Elmer 240Q elemental analyzer. Electrospray ionization mass spectra (ES-MS) were recorded on a LCQ system (Finnigan MAT, USA) using methanol as mobile phase. The spray voltage, tube lens offset, capillary voltage and capillary temperature were set at 4.50 KV, 30.00 V, 23.00 V and 200 ^{o}C, respectively, and the quoted *m/z* values are for the major peaks in the isotope distribution. ^1H NMR spectra were recorded on a Varian-500 spectrometer with DMSO [D_6] as solvent and tetramethylsilane (TMS) as an internal standard at 500 MHz at room temperature.

4.2. Syntheses of ligand and complexes

1,10-phenanthroline-5,6-dione [39] and ligand HDPIP [40] were prepared according to the methods in the literature.

4.2.1. [Ru(dmb)₂(HDPIP)](ClO₄)₂ (1). A mixture of cis-[Ru(dmb)₂Cl₂]·2H₂O [41] (0.288 g, 0.5 mmol) and HDPIP (0.212 g, 0.5 mmol) in ethanol (30 mL) was refluxed under argon for 8 h to give a clear red solution, and removed the solvent to about 10 mL. Upon cooling, a red precipitate was obtained by dropwise addition of saturated

11

aqueous $NaClO_4$ solution. The crude product was purified by column chromatography

on neutral alumina with a mixture of CH_3CN-toluene (3:1, v/v) as eluent. The red

band was collected. The solvent was removed under reduced pressure and a red

powder was obtained. Yield: 69%. Anal. Calc for $C_{51}H_{52}N_8Cl_2O_9Ru$: C, 56.04; H, 4.80;

N, 10.25%. Found: C, 56.51; H, 4.92; N, 9.86%. ^{1}H NMR (DMSO-d_6): δ 8.95 (d, 2H,

$J = 8.0$ Hz), 8.72 (d, 4H, $J = 8.5$ Hz), 8.29 (d, 1H, J = 6.0 Hz), 7.82 (d, 2H, J = 7.0 Hz),

7.73 (d, 2H, J = 6.5 Hz), 7.69 (d, 2H, $J = 6.0$ Hz), 7.38 (dd, 4H, $J = 5.0, J = 6.0$ Hz),

7.18 (d, 3H, $J = 6.0$ Hz), 2.55 (s, 6H), 2.45 (s, 6H), 1.48 (s, 9H), 1.36 (s, 9H). ES-MS

(CH_3CN): m/z 893.5 ($[M-2ClO_4-H]^+$), 447.4 ($[M-2ClO_4]^{2+}$).

4.2.2. [Ru(bpy)$_2$(HDPIP)](ClO$_4$)$_2$ (2). This complex was synthesized according to

the literature [40].

4.2.3. [Ru(phen)$_2$(HDPIP)](ClO$_4$)$_2$ (3). This complex was synthesized in a manner

identical to that described for complex **1**, with $[Ru(phen)_2Cl_2]·2H_2O$ [41] in place of

$[Ru(dmb)_2Cl_2]·2H_2O$. Yield: 70%. Anal. Calc for $C_{51}H_{44}N_8Cl_2O_9Ru$: C, 56.46; H, 4.09;

N, 10.33%. Found: C, 56.12; H, 4.48; N, 10.45%. ^{1}H NMR (DMSO-d_6): δ 8.99 (d, 2H,

$J = 6.5$ Hz), 8.77 (d, 4H, $J = 8.0$ Hz), 8.39 (s, 4H), 8.27 (d, 2H, J = 7.0 Hz), 8.10 (t,

4H, $J = 5.5$ Hz), 7.75-7.80 (m, 6H), 7.55 (s, 1H), 7.23 (s, 1H), 3.33 (s, 1H, H_{OH}), 1.48

(s, 9H), 1.36 (s, 9H). ESI-MS (CH_3CN): m/z 885.5 ($[M-2ClO_4-H]^+$), 443.4

($[M-2ClO_4]^{2+}$).

Caution: Perchlorate salts of metal compounds with organic ligands are potentially

explosive, and only small amounts of the material should be prepared and handled with great care.

4.3. In Vitro Cytotoxicity Assay

3-(4,5-dimethylthiazole)-2,5-diphenyltetraazolium bromide (MTT) assay procedures were used [42]. Cells were placed in 96-well microassay culture plates (8×10^3 cells per well) and grown overnight at 37 °C in a 5% CO_2 incubator. The tested compounds were then added to the wells to achieve final concentrations ranging from 10^{-6} to 10^{-4} M. Control wells were prepared by addition of culture medium (100 μL) and cisplatin was used as the positive control. The plates were incubated at 37 °C in a 5% CO_2 incubator for 48 h. Upon completion of the incubation, stock MTT dye solution (20 μL, 5 mg·mL^{-1}) was added to each well. After 4 h, buffer (100 μL) containing *N,N*-dimethylformamide (50%) and sodium dodecyl sulfate (20%) was added to solubilize the MTT formazan. The optical density of each well was then measured with a microplate spectrophotometer at a wavelength of 490 nm. The IC_{50} values were calculated by plotting the percentage viability versus concentration on a logarithmic graph and reading off the concentration at which 50% of cells remained viable relative to the control. Each experiment was repeated at least three times to obtain the mean values.

4.4. Apoptosis Assay by AO/EB Staining method

A549 cells were seeded onto chamber slides in six-well plates at a density of 2×10^5

cells per well and incubated for 24 h. The cells were cultured in RPMI 1640 supplemented with 10% of fetal bovine serum (FBS) and incubated at 37 °C and 5% CO_2. The medium was removed and replaced with medium (final DMSO concentration 0.05% v/v) containing complexes **1, 2** and **3** (12.5 μM) for 24 h. The medium was removed and the cells were washed with ice-cold PBS, and fixed with formalin (4%, w/v). Cell nuclei were counterstained with AO/EB solution (100 μg·mL^{-1} AO, 100 μg·mL^{-1} EB) for 10 min, then observed and imaged by fluorescence microscope (Nikon, Yokohama, Japan) with excitation at 350 nm and emission at 460 nm.

4.5. Cellular Uptake and Localization Studies

A549 cells were placed in 24-well microassay culture plates (4×10^4 cells per well) and grown overnight at 37 °C in a 5% CO_2 incubator. Complexes tested were then added to the wells. The plates were incubated at 37 °C in a 5% CO_2 incubator for 24 h. Upon completion of the incubation, the wells were washed three times with phosphate buffered saline (PBS), after removing the culture mediums from the wells. The cells were stained with 2-(4-amidinophenyl)-6-indolecarbamidine (DAPI) and visualized by fluorescence microscopy.

4.6. Reactive Oxygen Species levels Assays

A549 cells were seeded into six-well plates (Costar, Corning Corp, New York) at a density of 2×10^5 cells per well and incubated for 24 h. The cells were cultured in

RPMI 1640 supplemented with 10% of fetal bovine serum (FBS) and incubated at 37

°C and 5% CO_2. The medium was removed and replaced with medium (final DMSO

concentration, 0.05% v/v) containing complexes **1, 2** and **3** (6.25 μM) for 24 h. The

medium was removed again. The fluorescent dye 2',7'-dichlorodihydrofluorescein

diacetate (H_2DCF-DA) was added to the medium with a final concentration of 10 μM

to cover the cells. The treated cells were then washed with cold PBS–EDTA twice,

collected by trypsinization and centrifugation at 1,500 rpm for 5 min, and resuspended

in PBS–EDTA. Fluorescence intensity was determined by microplate analyzer

(THERMO Varioskan Flash, USA) with an excitation wavelength of 488 nm and

emission at 525 nm. The fluorescence intensity is calculated by the determined

fluorescence intensity minus the fluorescence intensity of the complexes in the

corresponding concentration.

4.7. Change of Mitochondrial Membrane Potential

A549 cells were treated for 24 h with complex in 12-well plates and were then

washed three times with cold PBS. The cells were detached with trypsin-EDTA

solution. Collected cells were incubated for 20 min with 1 μg/mL of JC-1 in culture

medium at 37 °C in the dark. Cells were immediately centrifuged to remove the

supernatant. Cell pellets were suspended in PBS and imaged by fluorescence

microscope and the red (525 nm) and green (590 nm) fluorescent intensity was

analyzed with microplate analyzer (THERMO Varioskan Flash, USA). The red and

green fluorescent intensity was calculated by the determined fluorescent intensity

minus the fluorescent intensity of the complexes in the corresponding concentration.

4.8. Cell Cycle Arrest by Flow Cytometry

A549 or BEL-7402 cells were seeded into six-well plates (Costar, Corning Corp, New York) at a density of 1×10^6 cells per well and incubated for 24 h. The cells were cultured in RPMI 1640 supplemented with fetal bovine serum (FBS, 10%) and incubated at 37 °C and 5% CO_2. The medium was removed and replaced with medium (final DMSO concentration 0.05% v/v) containing 12.5 μM complexes **1, 2** and **3**. After incubation for 24 h, the cell layer was trypsinized and washed with cold phosphate buffered saline (PBS) and fixed with 70% ethanol. Twenty μL of RNAse (0.2 mg/mL) and 20 μL of propidium iodide (0.02 mg/mL) were added to the cell suspensions and the mixtures were incubated at 37 °C for 30 min. The samples were then analyzed with a FACSCalibur flow cytometry. The number of cells analyzed for each sample was 10000 [43].

4.9. The Expression of Caspase, antiapoptotic and proapoptotic proteins

A549 cells were seeded in 3.5-cm dishes for 24 h and incubated with complex **3** at 6.25, 12.5 and 25 μM in the presence of 10% FBS. Then cells were harvested in lysis buffer. After sonication, the samples were centrifuged for 20 min at 13,000 g. The protein concentration of the supernatant was determined by BCA assay. Sodium dodecyl sulfate-polyacrylamide gel electrophoresis was done loading equal amount of proteins per lane. Gels were then transferred to poly (vinylidene difluoride)

membranes (Millipore) and blocked with 5% non-fat milk in TBST buffer for 1 h. Then the membranes were incubated with primary antibodies at 1:5,000 dilutions in 5% non-fat milk overnight at 4 °C, and washed four times with TBST for a total of 30 min. After which the secondary antibodies conjugated with horseradish peroxidase at 1:5,000 dilution for 1 h at room temperature and then washed four times with TBST. The blots were visualized with the Amersham ECL Plus western blotting detection reagents according to the manufacturer's instructions. To assess the presence of comparable amount of proteins in each lane, the membranes were stripped finally to detect the β-actin.

Acknowledgements

References

1. M. Markman, *Expert Opin Drug Saf*, 2003, 2, 597-607.

2. P.C. Bruijnincx, P.J. Sadler, *Curr. Opin. Chem. Biol.*, 2008, 12, 197-206.

3. G. B. Jiang, J. H. Yao, J. Wang, W. Li, B. J. Han, G. J. Lin, Y. Y. Xie, H. L. Huang and Y. J. Liu, *New J Chem*, 2014, 38, 2554-2563.

4. L. Xu, N. J. Zhong, Y. Y. Xie, G. J. Lin, H. L. Huang, G. B. Jiang and Y. J. Liu, *Plos One*, 2014, 9, e96082.

5. T. S. Kamatchi, P. Kalaivani, P. Poornima, V. V. Padma, F. R. Fronczek and K. Natarajan, RSC Adv, 2014, 4, 2004-2022.

6. G. J. Lin, G. B. Jiang, Y. Y. Xie, H. L. Huang, Z. H. Liang and Y. J. Liu, J. Biol. Inorg. Chem., 2013, 18, 873-882.

7. N. Busto, J. Valladolid, M. Martínez-Alonso, H. J. Lozano, F. A. Jalón, B. R. Manzano, A. M. Rodríguez, M. C. Carrión, T. Biver, J. M. Leal, G. Espino and B. García, *Inorg. Chem.*, 2013, 52, 9962-9974.

8. G. B. Jiang, Y. Y. Xie, G. J. Lin, H. L. Huang, Z. H. Liang and Y. J. Liu, *J. Photochem & Photobiol B: Biology*, 2013, 129, 48-56.

9. M. A. Sgambellone, A. David, R. N. Garner, K. R. Dunbar and C. Turro, *J. Am. Soc. Chem.*, 2013, 135, 11274-11282.

10. F. A. Egbewande, L. E. H. Paul, B. Therrien and J. Furrer, *Eur. J. Inorg. Chem.*, 2014, 7, 1174-1184.

11. A. Bergamo and G. Sava, *Dalton Trans*, 2007, 13, 1267-1272.

12. C. G. Hartinger, S. Zorbas-Seifried, M. A. Jakupec, B. Kynast, H. Zorbas and B.

K. Kepper, *J. Inorg. Biochem.*, 2006, 100, 891-904.

13. B. Biersack, M. Zoldakova, K. Effenberger and R. Schobert, *Eur. J. Med. Chem.*, 2010, 45, 1972-1975.

14. I. Łakomska, M. Fandzloch, T. Muzioł, T. Lis and J. Jezierska, *Dalton Trans*, 2013, 42, 6219-6226.

15. C. S. Devi, D. A. Kumar, S. S. Singh, N. Gabra, N. Deepika, Y. P. Kumar and S. Satyanarayana, *Eur. J. Med. Chem.*, 2013, 64, 410-421.

16. S. Betanzos-Lara, O. Novakova, R. J. Deeth, A. M. Pizarro, G. J. Clarkson, B. Liskova, V. Brabec, P. J. Sadler and A. Habtemariam, *J. Biol. Inorg. Chem.*, 2012, 17, 1033-1051.

17. S. Monro, J. Scott, A. Chouai, R. Lincoln, R. F. Zong and R. P. Thummel, *Inorg. Chem.*, 2010, 49, 2889-2990.

18. J. F. Kou, C. Qian, J. Q. Wang, X. Chen, L. L. Wang, H. Chao and L. N. Ji, *J. Biol. Inorg. Chem.* **2012**, *17*, 81-96.

19. T. S. Kamatchi, N. Chitrapriya, H. Lee, C. F. Fronczek, F. R. Fronzcek and K. Natarajan, *Dalton Trans*, 2012, 41, 2066-2077.

20. R. K. Gupta, R. Pandey, G. Sharma, R. Prasad, B. Koch, S. Srikrishna, P. Z. Li, Q. Xu and D. S. Pandey, *Inorg. Chem.*, 2013, 52, 3687-3798.

21. L. F. Tan, J. Liu, J. L. Shen, X. H. Liu, L. L. Zeng and L. H. Jin, *Inorg. Chem.*, 2012, 51, 4417-4419.

22. T. F. Chen, Y. N. Liu, W. J. Zheng, J. Liu and Y. S. Wong, *Inorg. Chem.*, 2010, 49, 6366-6368.

23. J. X. Zhang, K. L. Wong, W. K. Wong, N. K. Mak, D. W. J. Kwong and H. L. Tam, *Org. Biomol. Chem.*, 2011, 9, 6004-6010.

24. C. Qian, J. Q. Wang, C. L. Song, L. L. Wang, L. N. Ji and H. Chao, *Metallomics*, 2013, 5, 844-854.

25. G. B. Jiang, J. H. Yao, J. Wang, W. Li, B, J, Han, Y. Y. Xie, G. J. Lin, H. L. Huang, Y. J. Liu, *New J Chem.*, 2014, 38, 2554-2563.

26. G. J. Lin, Z. Z. Li, J. H. Yao, H. L. Huang, Z. H. Liang, Y. Y. Xie and Y. J. Liu, *Aust. J. Chem.*, 2013, 66, 555-563.

27. Y. Y. Xie, Z. Z. Li, G. J. Lin, H. L. Huang, X. Z. Wang, Z. H. Liang, G. B. Jiang and Y. J. Liu, *Inorg. Chimca. Acta.*, 2013, 405, 228-234.

28. P. Kalaivani, R. Prabhakaran, P. Poornima, R. Huang, V. Hornebecq, F. Dallemer, V. V. Padmab, K. Natarajan, *RSC Adv.*, 2013, 3, 20363-20378.

29. T. Bugarcic, O. Nováková, A. Halámiková, L. Zerzánková, O. Vrána, L. Kašpárková, A. Habtemariam, S. Parsons, P. J. Sadler and V. Brabec, *J. Med. Chem.*, 2008, 51, 5310-5319.

30. U. Schatzschneider, J. Niesel, I. Ott, R. Gust, H. Alborzinia and S. Wolfl, *ChemMedChem*, 2008, 3, 1104-1109.

31. Y. Y. Xie, H. L. Huang, J. H. Yao, G. J. Lin, G. B. Jiang and Y. J. Liu, *Eur. J. Med. Chem.,* 2013, 63, 603-610.

32. C. A. Puckett and J. K. Barton, *Biochemistry*, 2008, 47, 11711-11716.

33. C. A. Puckett and J. K. Barton, *J. Am. Soc. Chem.*, 2007, 129, 46-47.

34. E. Cadenas, K. J. A. Davies, *Free Radical Biol. Med.*, 2000, 29, 222-230.

35. A. Kawiak, J. Zawacka-Pankau, A. Wasilewska, G. Stasilojc, J. Bigda, E. Lojkowska, *J. Nat. Prod.*, 2012, 75, 9-14.

36. L. R. Silveira, L. Pereira-Da-Silva, C. Juel, Y. Hellsten, *Free Radic. Biol. Med.*, 2003, 35, 455-464.

37. K. Ito, A. Hirao, F. Arai, K. Takubo, S. Matsuoka, K. Miyamoto, M. Ohmura, K. Naka, K. Hosokawa, Y. Ikeda, T. Suda, *Nat. Med.*, 2006, 12, 446-451.

38. D. E. Merry and S. J. Korsmeyer, *Annu. Rev. Neurosci.*, 1997, 20, 245-267.

39. W. Paw and R. Eisenberg, *Inorg. Chem.*, 1997, 36, 2287-2293.

40. F. Lachaud, A. Quaranta, Y. Pellegrin, P. Dorlet, M. E. Charlot, S. U. W. Leibl, A. Aukauloo, *Angew. Chem. Int. Ed.*, 2005, 44, 1536-1540.

41. B. P. Sullivan, D. J. Salmon, T. J. Meyer, *Inorg. Chem.*, 1978, 17, 3334-3341.

42. T. Mosmann, *J. Immunol. Methods*. 1983, 65, 55-63.

43. K. K. Lo, T. K. Lee, J. S. Lau, W. L. Poon and S. H. Cheng, *Inorg. Chem.*, 2008, 47, 200-208.

Captions for Schemes and Figures

Scheme 1 Synthetic route of ligand and complexes **1, 2** and **3**

Fig. 1 A549 cells were stained by AO/EB and observed under fluorescence microscopy. A549 cells (a) exposure to 12.5 μM of complexes **1** (b), **2** (c) and **3** (d) at 37 $^{\circ}$C and 5% CO_2 for 24 h. cells in Liv, Apo and Nec are living, apoptotic and necrotic cells.

Fig. 2 Images of A549 cells exposure to 25 μM of complexes **1** (A), **2** (B), **3** (C) and DAPI-stained at 37 $^{\circ}$C for 24 h.

Fig. 3 Effects on ROS generation induced by 6.25 μM of complexes **1**, **2** and **3** in A549 cells. Data are the mean fluorescene intensity ± SD (data in brackets) calculated from three independent experiments.

Fig. 4 Assay of A549 cells mitochondrial membrane potential with JC-1 as fluorescence probe staining method. a: control, b, c and d exposed to 12.5 μM of complexes **1**, **2** and **3** for 24 h.

Fig. 5 Assay of A549 cells mitochondrial membrane potential with JC-1 as fluorescence probe staining method. A549 cells (■) exposed to 12.5 or 25 μM of complexes **1** (■), **2** (■) and **3** (■) for 24 h.

Fig. 6 a) Cell cycle distribution of A549 cells exposure to 12.5 μM of complexes **1**, **2** and **3**. b) BEL-7402 cells exposure to 12.5 μM of complex **1** for 24 h.

Fig. 7 Roles of Bcl-2 and caspase family members in apoptosis induced by complex **3**. Cells were treated with indicated concentrations of complex **3** for 24 h and the expression levels of the apoptosis-related proteins were examined by western

blot.

Table 1 The IC$_{50}$ values of complexes **1**, **2** and **3** against BEL-7402, A549, MG-63 and SK-BR-3 cell lines.
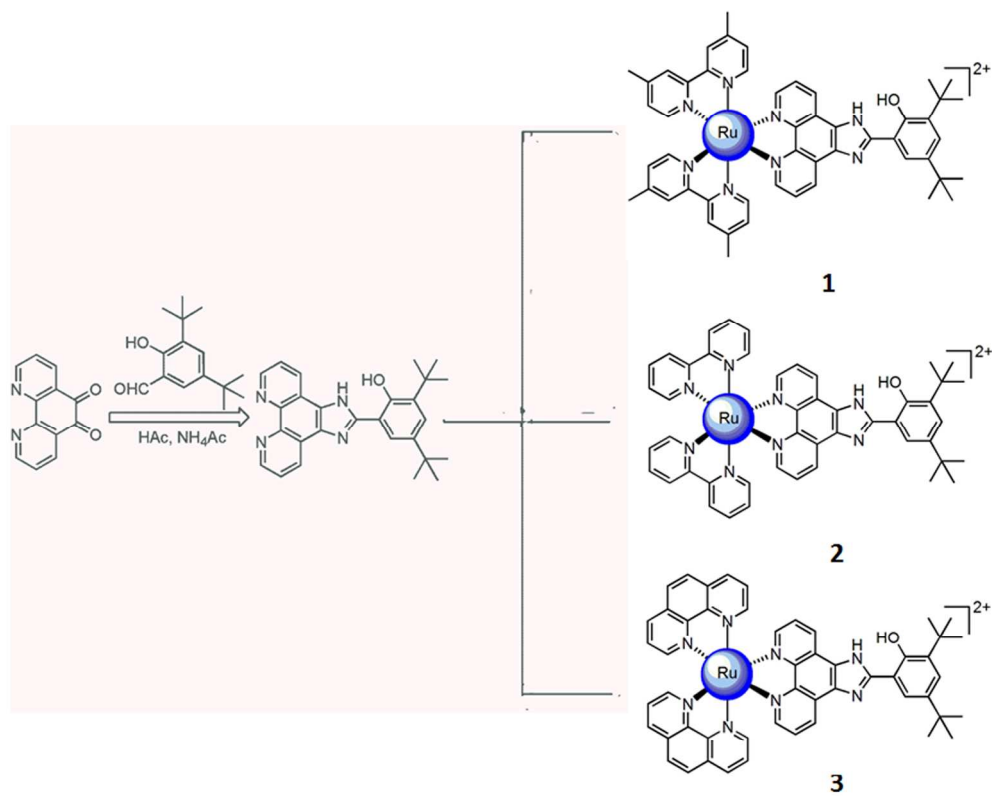
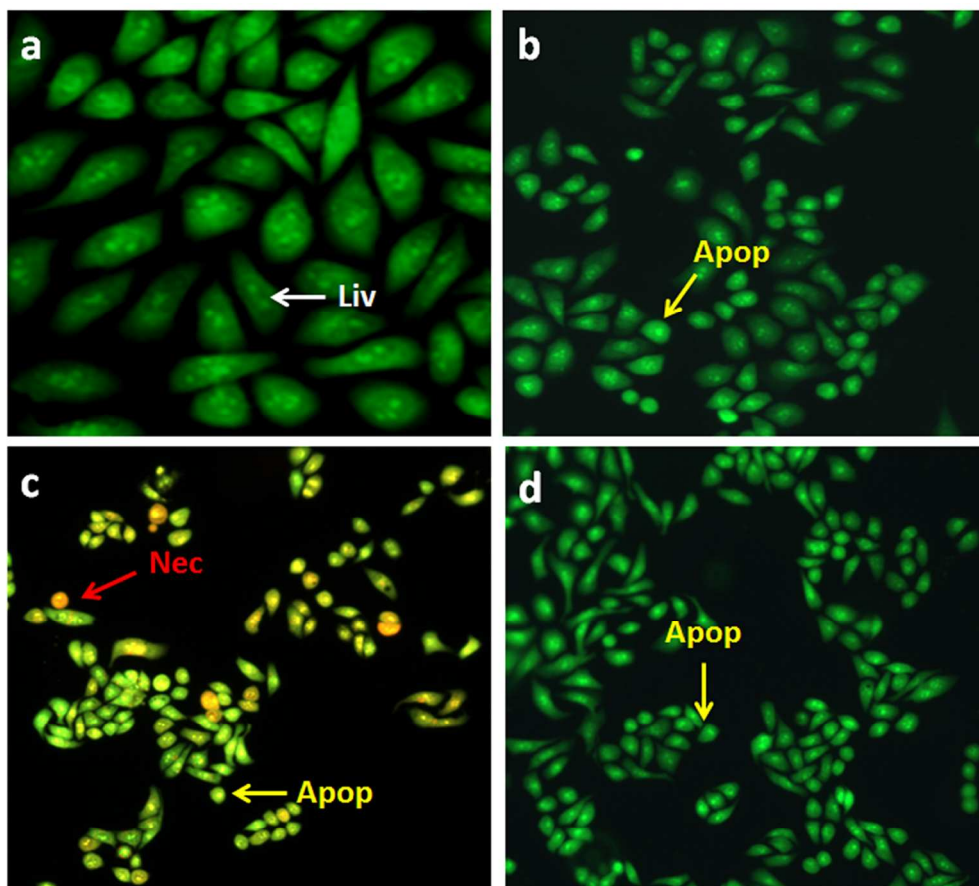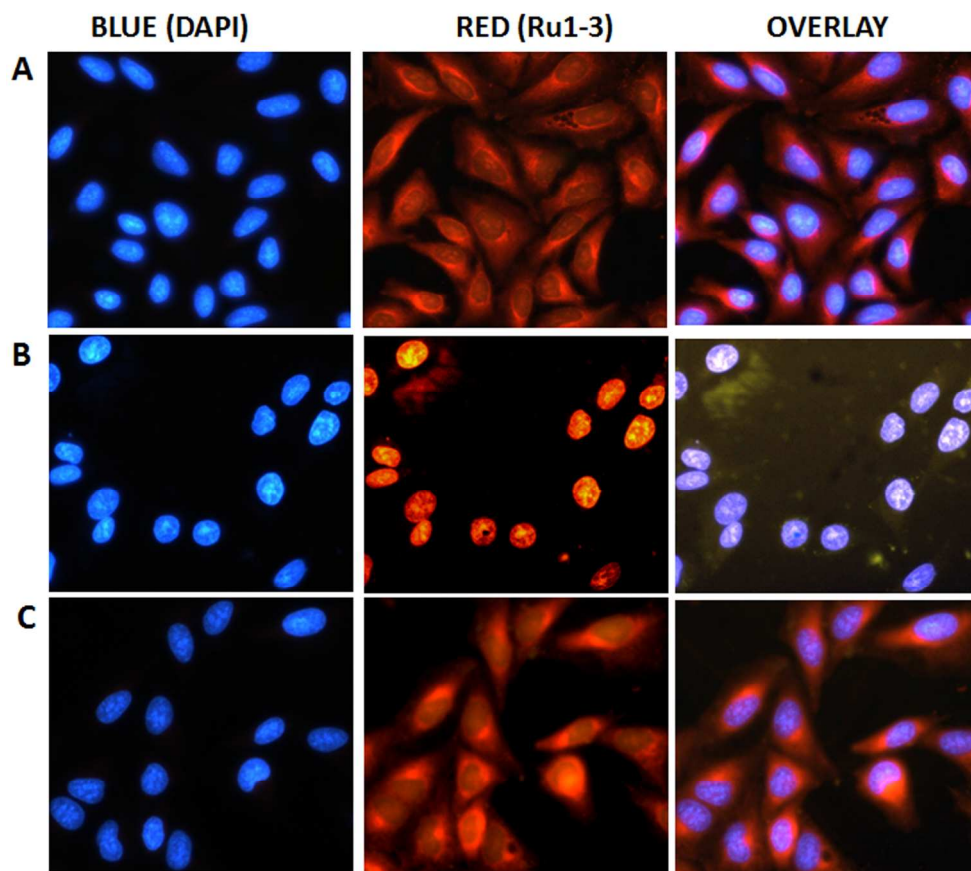Scheme 1 Synthetic route of ligand and complexes **1**, **2** and **3**.

143x119mm (300 x 300 DPI)

Fig. 1 A549 cells were stained by AO/EB and observed under fluorescence microscopy. A549 cells (a) exposure to 12.5 µM of complexes **1** (b), **2** (c) and **3** (d) at 37 $^{\circ}$C and 5% CO_2 for 24 h. cells in Liv, Apo and Nec are living, apoptotic and necrotic cells.

283x291mm (300 x 300 DPI)

Fig. 2 Images of A549 cells exposure to 25 µM of **complexes 1 (A)**, 2 (B), **3 (C)** and DAPI-stained at 37 °C for 24 h.
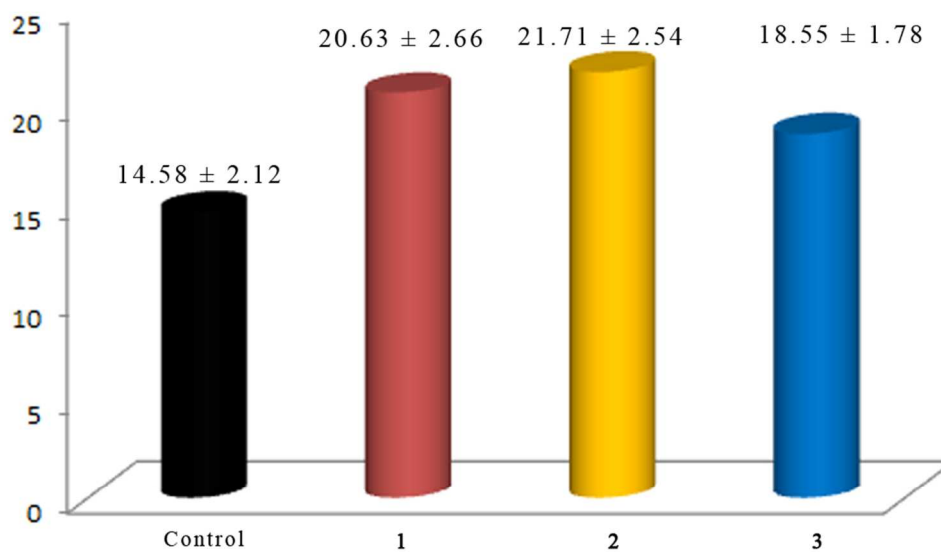
308x299mm (300 x 300 DPI)

Fig. 3 Effects on ROS generation induced by 6.25 μM of complexes **1**, **2** and **3** in A549 cells. Data are the mean fluorescene intensity ± SD calculated from three independent experiments.

86x60mm (300 x 300 DPI)

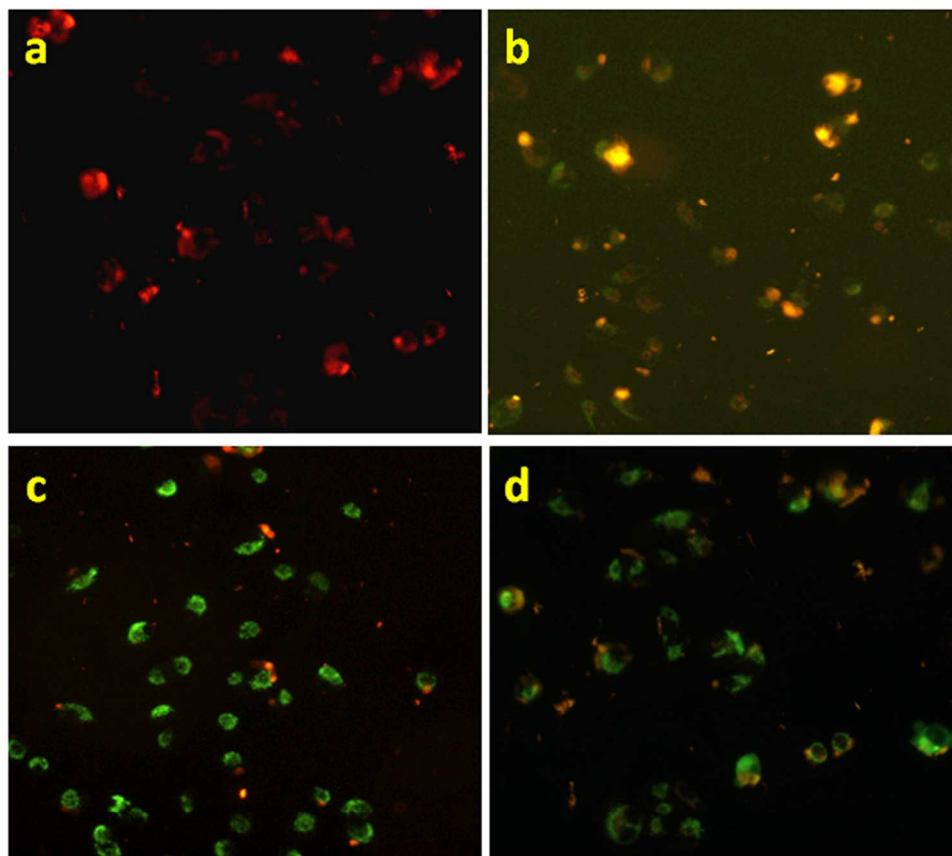Fig. 4 Assay of A549 cells mitochondrial membrane potential with JC-1
as fluorescence probe staining method. a: control, b, c and d exposed to 12.5
μM of complexes **1**, **2** and **3** for 24 h.
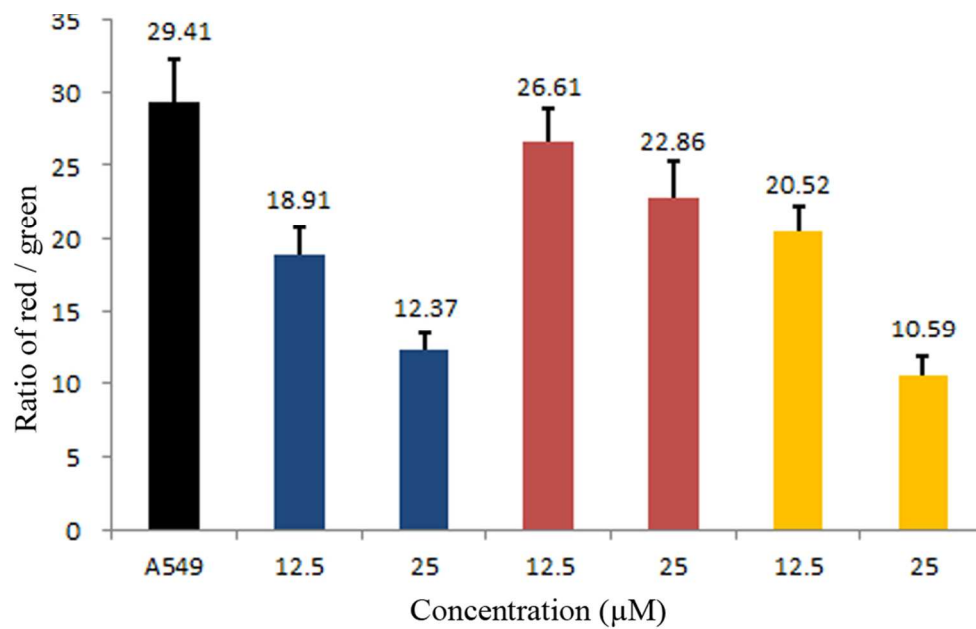
297x299mm (300 x 300 DPI)

Fig. 5 Assay of A549 cells mitochondrial membrane potential with JC-1 as fluorescence probe staining method. A549 cells (■) exposed to 12.5 or 25 μM of complexes **1** (■), **2** (■) and **3** (■) for 24 h.
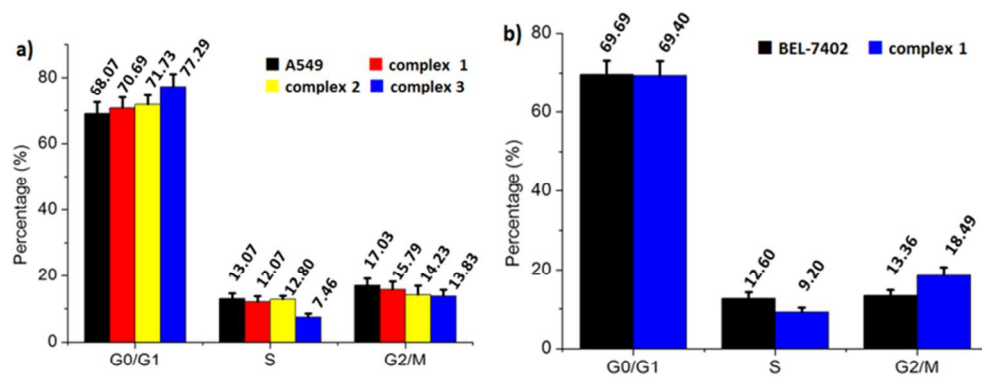
89x66mm (300 x 300 DPI)

Fig. 6 a) Cell cycle distribution of A549 cells exposure to 12.5 µM of complexes **1**, **2** and **3**. b) BEL-7402 cells exposure to 12.5 µM of complex **1** for 24 h.
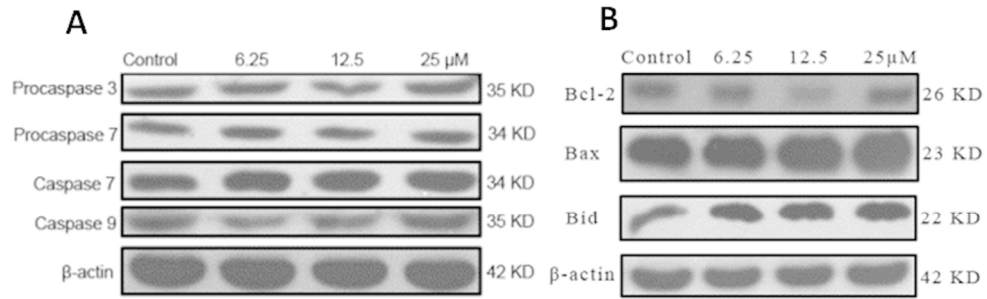
156x70mm (300 x 300 DPI)

Fig. 7 Roles of Bcl-2 and caspase family members in apoptosis induced by complex **3**. Cells were treated with indicated concentrations of complex **3** for 24 h and the expression levels of the apoptosis-related proteins were examined by western blot.

164x70mm (300 x 300 DPI)

Table 1 The IC$_{50}$ values of complexes **1**, **2** and **3** against BEL-7402, A549, MG-63 and SK-BR-3 cell lines.

Complex	IC$_{50}$ (µM)			
	BEL-7402	A549	MG-63	SK-BR-3
1	13.6 ± 1.2	8.6 ± 1.1	21.7 ± 2.7	16.8 ± 2.2
2	20.8 ± 1.6	13.3 ± 1.1	14.9 ± 1.5	13.2 ± 1.3
3	13.8 ± 1.4	7.3 ± 1.0	15.1 ± 1.2	13.1 ± 1.2
Cisplatin	11.4 ± 1.2	7.3 ± 1.4	6.6 ± 0.5	6.8 ± 0.8